

REPORT DOCUMENTATION PAGE

Form Approved
OMB No. 0704-0188

Public reporting burden for this collection of information is estimated to average 1 hour per response, including the time for reviewing instructions, searching existing data sources, gathering and maintaining the data needed, and completing and reviewing the collection of information. Send comments regarding this burden estimate or any other aspect of this collection of information, including suggestions for reducing this burden to Washington Headquarters Services, Directorate for Information Operations and Reports, 1215 Jefferson Davis Highway, Suite 1204, Arlington, VA 22202-4302, and to the Office of Management and Budget, Paperwork Reduction Project (0704-0188), Washington, DC 20503.

PLEASE DO NOT RETURN YOUR FORM TO THE ABOVE ADDRESS.

1. REPORT DATE (DD-MM-YYYY)		2. REPORT TYPE Journal Article		3. DATES COVERED	
4. TITLE AND SUBTITLE A Note on Analyzing Nonlinear and Nonstationary Ocean Wave Data				5a. CONTRACT NUMBER	
				5b. GRANT NUMBER	
				5c. PROGRAM ELEMENT NUMBER	
6. AUTHOR(S) Paul A. Hwang, Norden E. Hyang and David W. Wang				5d. PROJECT NUMBER	
				5e. TASK NUMBER	
				5f. WORK UNIT NUMBER	
7. PERFORMING ORGANIZATION NAME(S) AND ADDRESS(ES) Naval Research Laboratory Oceanography Division Stennis Space Center, MS 39529-5004				8. PERFORMING ORGANIZATION REPORT NUMBER NRL/JA/7330/02/0078	
9. SPONSORING/MONITORING AGENCY NAME(S) AND ADDRESS(ES) Office of Naval Research 800 N. Quincy St. Arlington, VA 22216-5660				10. SPONSOR/MONITOR'S ACRONYM(S) ONR	
				11. SPONSOR/MONITOR'S REPORT NUMBER(S)	
12. DISTRIBUTION/AVAILABILITY STATEMENT Approved for public release; distribution is unlimited					
13. SUPPLEMENTARY NOTES <div style="text-align: right; font-size: 2em; font-weight: bold;">20040604 121</div>					
14. ABSTRACT The Huang—Hilbert transformation (HHT, composed of empirical mode decomposition and Hubert transformation) can be applied to calculate the spectrum of nonlinear and nonstationary signals. The superior temporal and frequency resolutions of the HHT spectrum are illustrated by several examples in this article. The HHT analysis interprets wave nonlinearity in terms of frequency modulation instead of harmonic generation. The resulting spectrum contains much higher spectral energy at low frequency and sharper drop off at high frequency in comparison with the spectra derived from Fourier-based analysis methods (e.g. FFT and wavelet techniques). For wind generated waves, the spectral level of the Fourier spectrum is about two orders of magnitude smaller than that of the HHT spectrum at the first subharmonic of the peak frequency. The resulting average frequency as defined by the normalized first momentum of the spectrum is about 1.2 times higher in the Fourier-based spectra than that of the HHT spectrum.					
15. SUBJECT TERMS Nonlinear; Nonstationary; Huang—Hilbert transformation; Empirical mode decomposition; FFT; Wavelet; Frequency modulation; Wave spectrum					
16. SECURITY CLASSIFICATION OF:			17. LIMITATION OF ABSTRACT	18. NUMBER OF PAGES	19a. NAME OF RESPONSIBLE PERSON
a. REPORT	b. ABSTRACT	c. THIS PAGE			Paul Hwang
Unclassified	Unclassified	Unclassified	SAR	6	19b. TELEPHONE NUMBER (Include area code) 228-688-4708

A note on analyzing nonlinear and nonstationary ocean wave data

Paul A. Hwang^{a,*}, Norden E. Huang^b, David W. Wang^a

^aOceanography Division, Naval Research Laboratory, Stennis Space Center, MS 39529-5004, USA

^bEarth Science Branch, NASA, Goddard Space Flight Center, Greenbelt, MD 20770, USA

Received 8 January 2003; accepted 10 November 2003

Abstract

The Huang–Hilbert transformation (HHT, composed of empirical mode decomposition and Hilbert transformation) can be applied to calculate the spectrum of nonlinear and nonstationary signals. The superior temporal and frequency resolutions of the HHT spectrum are illustrated by several examples in this article. The HHT analysis interprets wave nonlinearity in terms of frequency modulation instead of harmonic generation. The resulting spectrum contains much higher spectral energy at low frequency and sharper drop off at high frequency in comparison with the spectra derived from Fourier-based analysis methods (e.g. FFT and wavelet techniques). For wind generated waves, the spectral level of the Fourier spectrum is about two orders of magnitude smaller than that of the HHT spectrum at the first subharmonic of the peak frequency. The resulting average frequency as defined by the normalized first momentum of the spectrum is about 1.2 times higher in the Fourier-based spectra than that of the HHT spectrum.

Published by Elsevier Ltd.

Keywords: Nonlinear; Nonstationary; Huang–Hilbert transformation; Empirical mode decomposition; FFT; Wavelet; Frequency modulation; Wave spectrum

1. Introduction

Fourier-based spectral analysis methods have been widely used for studying random waves. One major weakness of the Fourier-based spectral analysis methods is the assumption of *linear* superposition of wave components. As a result, the energy of a nonlinear wave is spread into many harmonics, which are phase-coupled via the nonlinear dynamics inherent in ocean waves. In addition to the nonlinearity issue, strictly speaking Fourier spectral analysis should be used for *periodic* and *stationary* processes only. Wave propagation in the ocean is certainly neither stationary nor periodic.

Recently, Norden Huang and his colleagues developed a new analysis technique, the Huang–Hilbert Transformation (HHT). Through analytical examples, they demonstrated the superior frequency and temporal resolutions of HHT for analyzing nonstationary and nonlinear signals [1,2]. The confidence band of the resulting HHT spectrum is discussed in great detail by Huang et al. [3]. A brief description of the HHT analysis technique is presented in Section 2. Using the HHT analysis, the physical interpretation of nonlinearity is

frequency modulation, which is fundamentally different from the commonly accepted concept associating nonlinearity with harmonic generation. Huang et al. argued that harmonic generation is caused by the perturbation method used in solving the nonlinear equation governing the physical processes, thus the harmonics are produced by the mathematical tools used for the solution rather than a true physical phenomenon.

In Section 3, we examine the spectrum of wind generated waves derived from HHT analysis and compare the results with those obtained by Fourier-based techniques (wavelet and FFT algorithms). The wavelet technique is based on Fourier spectral analysis but with adjustable frequency-dependent window functions, generally called mother wavelets, to provide temporal/spatial resolution for nonstationary signals. As expected, the Fourier-based analysis interprets wave nonlinearity in terms of harmonic generation, thus the spectral energy leaks to higher frequency components. The HHT interprets wave nonlinearity as frequency modulation and the spectral energy remains near the base frequencies. As a result, the HHT spectral level is considerably higher than the Fourier-based spectra in the lower frequency region. In the higher frequency portion, the HHT spectrum shows a steeper dropoff than the Fourier-based spectra. These differences in the wave spectral

* Corresponding author. Fax: +1-228-688-5379.

E-mail address: paul.hwang@nrlssc.navy.mil (P.A. Hwang).

properties affect many engineering applications such as the frequency response of marine structures. Based on the interpretation of nonlinearity as frequency modulation, the mean frequency of ocean wave spectrum is about 1.2 times lower than that given by Fourier analysis. A summary is given in Section 4.

2. The Huang–Hilbert spectral analysis

Hilbert transformation was introduced to water wave analysis in the 80s [4–6]. A main application of the Hilbert analysis is to derive local wavenumber in a spatial series or instantaneous frequency in a time series. To use the Hilbert transformation, proper preprocessing of the signals is very critical. Large errors in the computed local frequency or wavenumber can occur when small wavelets are riding on longer waves. A quantitative illustration of the riding wave problem has been discussed in great details by Huang et al. [1] and will not be repeated here. The common approach in the past to alleviate this problem is to apply low pass filter to the signal prior to Hilbert transformation. The determination of the low pass frequency is somewhat subjective, and

the signals removed may contain the information of nonlinearity, which are frequently the features to be studied. Furthermore, simple low-pass operation may not eliminate the riding wave problem.

The key ingredient in the HHT is empirical mode decomposition (EMD) designed to reposition the riding waves at the mean water level. Extensive discussions on the EMD have been given by Huang et al. [1,2]. The main idea is to find the trend that can represent the mean local average so that riding waves can be identified. The EMD method uses the point-by-point average of the signal envelopes for the local mean. The difference between the original signal and the local mean represents a mode of the signal. The local mean may also contain riding waves, and the mode decomposition process continues until no riding waves exist in the local mean signal. The process is called ‘sifting’ by Huang et al. [1]. From experience, even for very complicated random signals, a time series can usually be decomposed into a relatively small number of modes, $M < \log_2 N$. Each mode is free of riding waves, thus the Hilbert transformation yields accurate local frequency of the mode. The spectrum of the original signal can be obtained by the sum of the Hilbert spectra of all modes. Extensive tests have been carried out by Huang et al. [1,2].

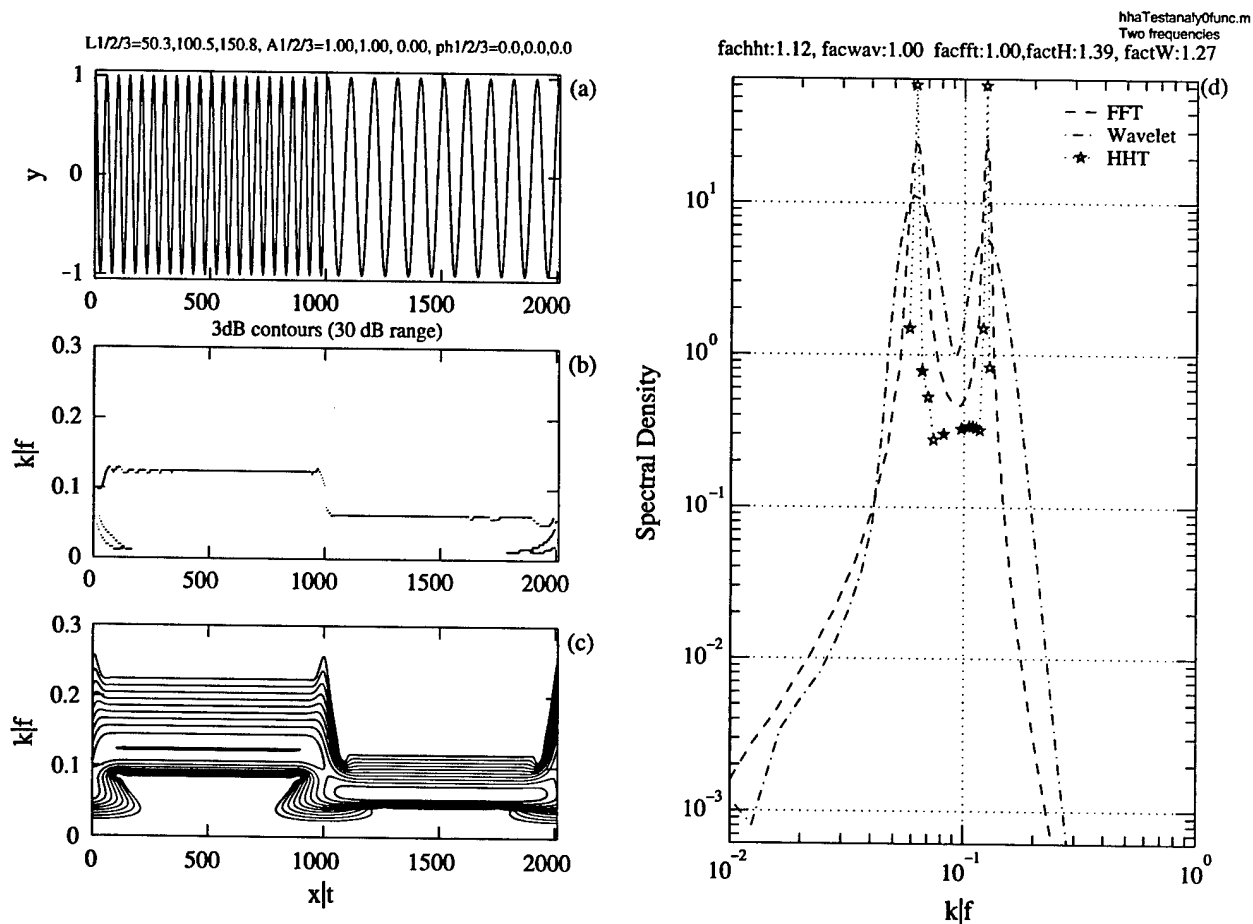


Fig. 1. (a) Simple sinusoidal oscillations with the frequency (f) or wavenumber (k) of the first half double that of the second half, (b) the computed HHT spectrum, (c) the computed wavelet spectrum, and (d) a comparison of the spatially or temporally averaged spectra computed by FFT, wavelet and HHT methods. The frequency (wavenumber) is normalized by the Nyquist value.

Here we present three cases to illustrate the superior resolutions of the HHT spectrum.

Case 1 is an example of an ideal time (t) or space (x) series of sinusoidal oscillations of constant amplitude, the frequency (f) or wavenumber (k) of the first half of the signal is twice that of the second half (Fig. 1a). The spectra computed by the HHT and wavelet techniques are displayed in Fig. 1(b) and (c), respectively. The HHT spectrum yields very precise frequency resolution and also high temporal resolution in identifying the sudden change of signal frequency at about the half point of the time series. In comparison, the wavelet spectrum has only a mediocre temporal resolution of the frequency change. There is also a serious leakage problem and the spectral energy of the simple oscillations spreads over a broad frequency range. Unless specified otherwise, the spectral contours plotted in the figures presented in this article are 3 dB (0.3 in logarithmic scale, approximately a factor of two) apart and covers a 30-dB range. For the example given in Fig. 1c, the 3 dB contour near the spectral peak extends between 0.8 and 1.2 times of the spectral peak frequency for the wavelet spectrum. In contrast, the HHT spectral energy is pretty much contained at the two spectral peak frequencies, the spectral density of the next frequency

bin is at least 10 dB down, as estimated by the marginal spectrum averaged over the whole time sequence (Fig. 1d). The spectral peak discrimination power can be quantified by the ratio between the spectral peaks and the neighboring spectral valleys. For HHT, this number is 23 dB, the FFT analysis gives 16 dB, and wavelet 8 dB. Also noticeable in Fig. 1d is the unequal spectral densities at the two peaks of the wavelet spectrum caused by the application of frequency-dependent windows in the wavelet analysis. The spectral density at the second frequency component is only about 60% of the spectra density at the first frequency component.

Case 2 is a single cycle sinusoidal oscillation occurring at the middle of the otherwise quiescent signal stream (Fig. 2a). The frequency of the single cycle oscillation is 1/32 cycles per second. The precise temporal resolution of the HHT method is clearly demonstrated by the sharp rise and fall of the HHT spectrum coincident with the transient signal as shown in Fig. 2b. In comparison, the wavelet spectrum is much more smeared both in the frequency and temporal resolutions (Fig. 2c). The marginal spectrum derived from the HHT analysis shows a much sharper frequency definition of the single oscillating cycle as compared to the wavelet and FFT spectra (Fig. 2d).

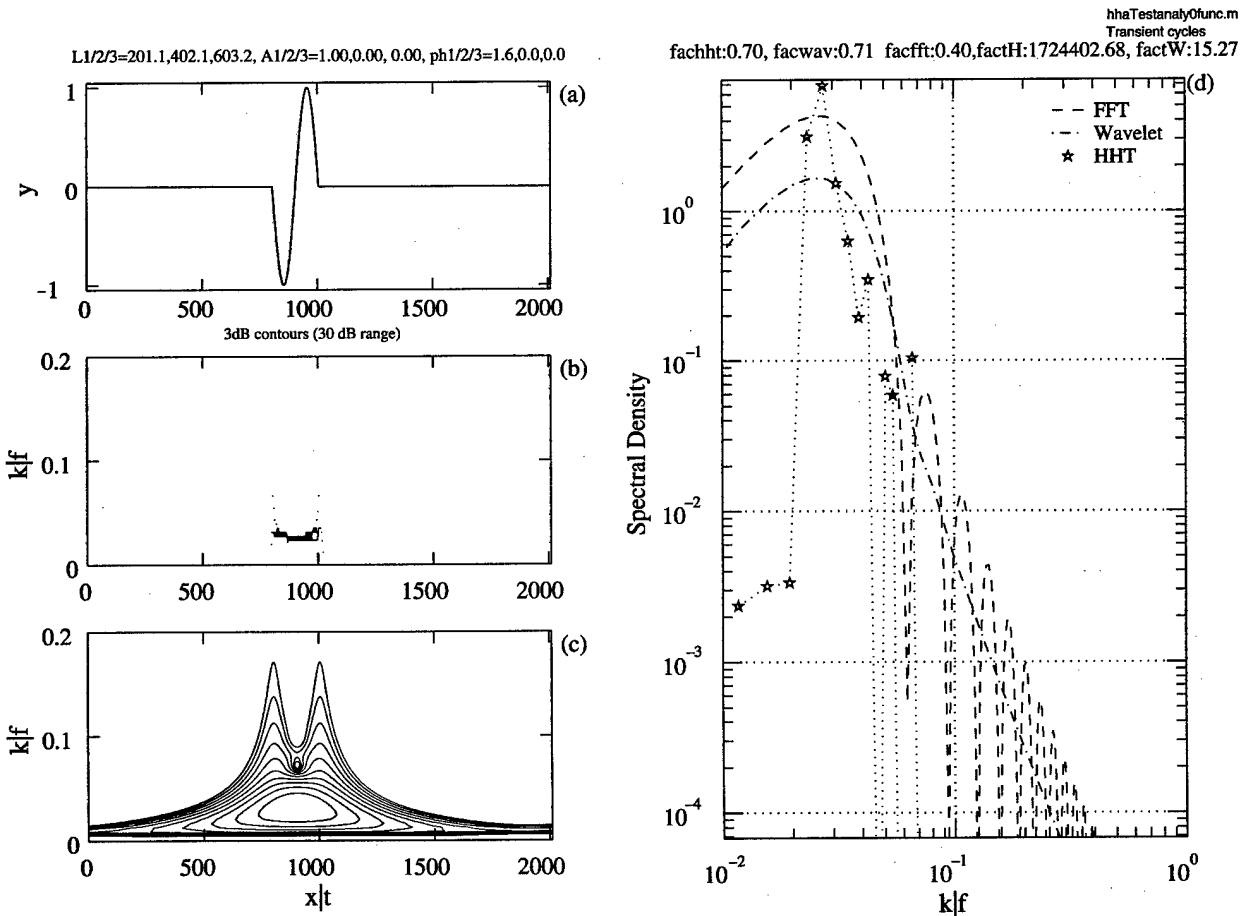


Fig. 2. Same as Fig. 1 but for a transient sinusoidal wave of one cycle.

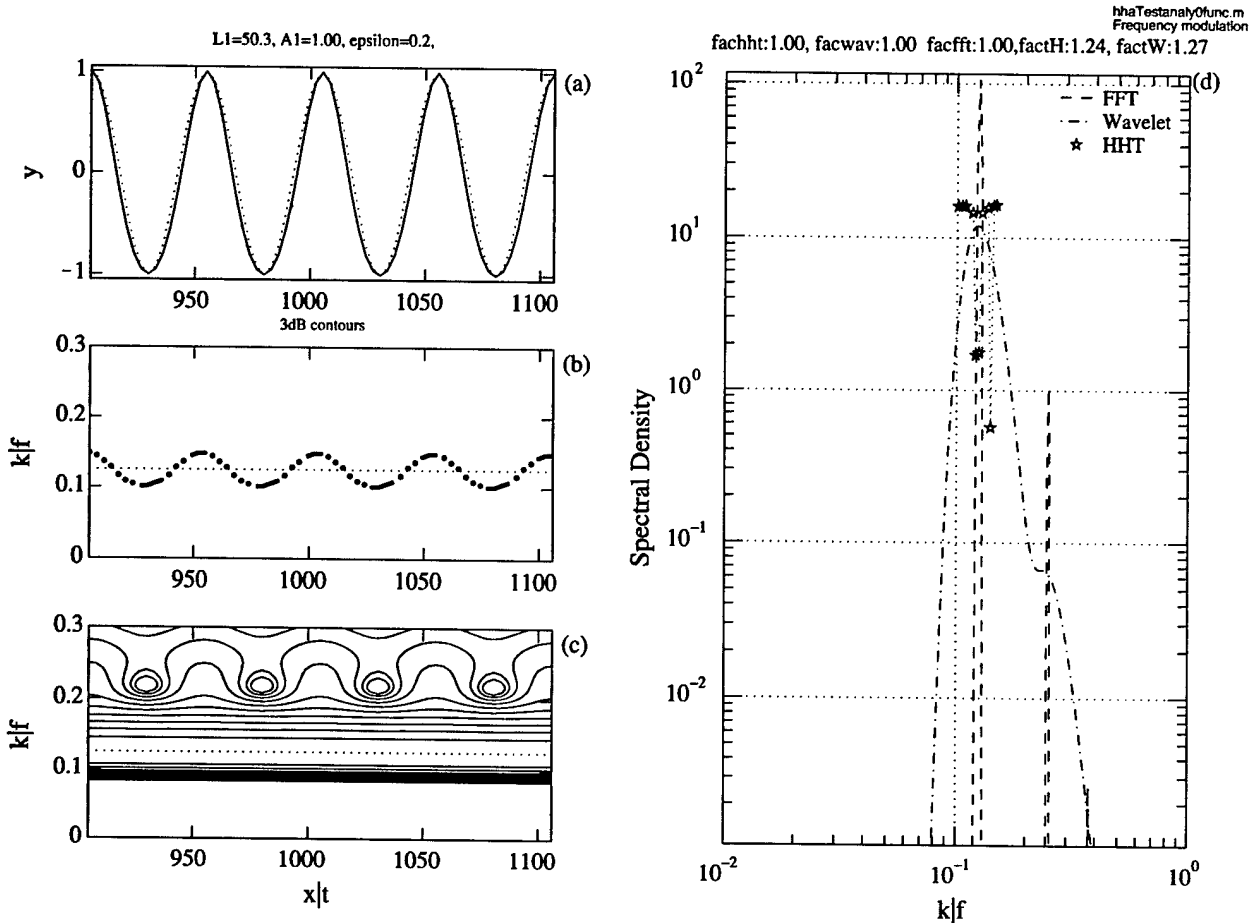


Fig. 3. Same as Fig. 1 but for a signal with modulated frequency, $y(t) = a \cos(\omega t + \epsilon \sin \omega t)$. The unmodulated mean frequency is shown by dotted lines in (b) and (c) for reference.

Case 3 is a sinusoidal function, y , with its oscillating frequencies subject to periodic modulation (Fig. 3a)

$$y(t) = a \cos(\omega t + \epsilon \sin \omega t), \tag{1}$$

where a is the amplitude, ω is the angular frequency and ϵ is a small perturbation parameter. This is the exact solution for the nonlinear differential equation [1].

$$\frac{d^2 y}{dt^2} + (\omega + \epsilon \omega \cos \omega t)^2 y - (1 - x^2)^{0.5} \epsilon \omega^2 \sin \omega t = 0. \tag{2}$$

If the perturbation method is used to solve Eq. (2), the solution to the first order of ϵ is

$$y_1(t) = \cos \omega t - \epsilon \sin^2 \omega t = \cos \omega t - \epsilon \left[\frac{1}{2} (1 - \cos 2\omega t) \right]. \tag{3}$$

The HHT spectrum (Fig. 3b) correctly reveals the nature of oscillatory frequencies of the exact solution Eq. (1). In contrast, the wavelet spectrum (Fig. 3c) shows a dominant component at the base frequency and periodic oscillations of the second harmonic component. In the marginal spectrum (Fig. 3d), the HHT analysis shows that the spectral energy is confined in the narrow frequency band surrounding the base frequency, which reflects the nature of frequency

modulation of the nonlinear system Eq. (2). Both FFT and wavelet analysis spread the spectral energy into higher frequencies as a result of harmonic generation by Fourier decomposition of a nonlinear signal. The Fourier decomposition turns out to be a perfect match for representing the perturbation solutions such as Eq. (3). In this example, we have chosen $\epsilon = 1/5$, so the spectral density of the second harmonic is 1/100 of the primary component, which is accurately reproduced by the FFT spectrum. The wavelet spectrum under-predicts the magnitude of the second harmonic by about 40%, similar to the results in Case 1 (Fig. 1d).

The three examples shown above illustrate the excellent temporal (spatial) and frequency (wavenumber) resolution of the HHT method for processing nonlinear and nonstationary signals. Many more demonstration cases are presented by Huang et al. [3,4].

3. Spectrum of wind generated waves

Here we investigate the impact on the wind wave spectral functions using different spectral analysis techniques described in Section 2. The wave record is acquired by

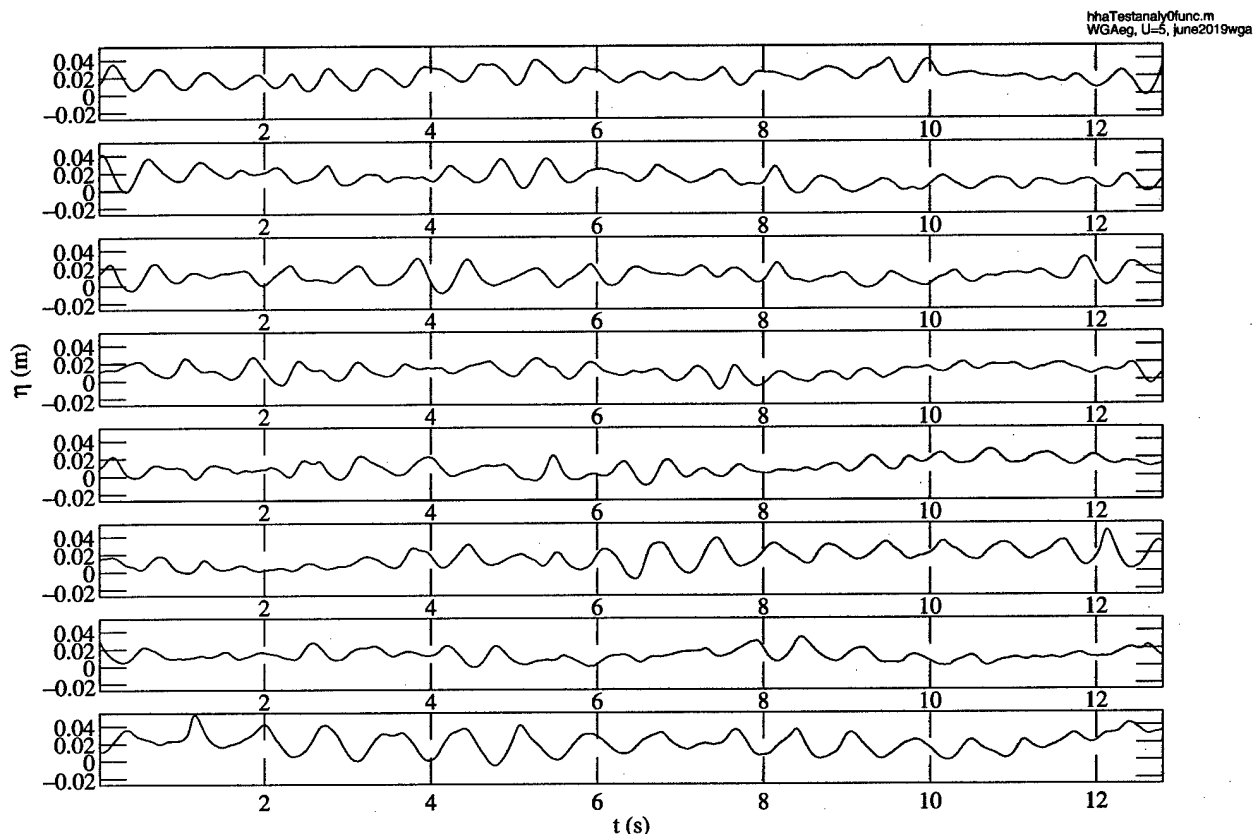


Fig. 4. Examples of the time series of wind-generated waves used for spectral comparison, the average wind speed is about 5 m s^{-1} . The data are measured by a fast response wire gauge sampled at 50 Hz.

a fast-response wire gauge [7] during a test deployment in a canal (approximately 100 m wide and 1000 m long). The data are sampled at 50 Hz, the wind condition is light and variable with a range between 0 to 5 m s^{-1} . Fig. 4 displays examples of the wave record showing the typical quasi-random time series of wind waves rich with group structure. Visual inspection suggests that the peak period is somewhat longer than 0.6 s and one expects considerable lower frequency energy associated with the wave groups. The number of carrier waves in a group ranges mostly between 3 and 10.

Wave spectra are calculated by the three methods using 20 segments of the wave record, each segment contains 640 data points (12.8 s). For the Fourier spectrum, the mean of the 20 raw spectra is further running-averaged across nine frequency bins, resulting in the final spectrum with 360 degrees of freedom. For the HHT and wavelet spectra, each data segment produces a temporal variation of the wave spectrum. The average over time gives the marginal (1D) spectrum. The procedure is repeated for the 20 segments to obtain the final average HHT and wavelet frequency spectra. Fig. 5 compares the spectra derived from these three different processing procedures. The similarities and differences of the spectral properties are described below.

The peak frequencies of the three spectra are close to 1.9 Hz for average wind speed $U = 2 \text{ m s}^{-1}$ (Fig. 5a)

and 1.4 Hz at $U = 5 \text{ m s}^{-1}$ (Fig. 5b). A secondary peak near the frequency component with minimum phase speed, $f_m = 13.6 \text{ Hz}$, is very prominent in the Fourier spectrum. The secondary peak is still discernible in the wavelet spectrum, but it is buried in the noise of the HHT spectrum.

Overall, the wavelet spectrum represents a smoothed version of the Fourier spectrum. The two Fourier-based spectra produce essentially similar results. Differences between the two spectra can be attributed to the degree of freedom, which is considerably higher in the wavelet analysis through the multiple windowing procedure.

The HHT spectrum differs from the other two Fourier-based spectra in two main areas. The spectral density at the low frequency portion is considerably higher in the HHT spectra, but near the peak and at higher frequencies the reverse is true. As we have emphasized in Section 2, this result is expected because the different interpretations of wave nonlinearity between HHT and Fourier-based methods. Fourier-based techniques always decompose a nonlinear wave into its base frequency and higher harmonics, therefore some spectral energy in the higher frequencies are leaked from their lower frequency sub-harmonics. There are higher order spectral processing methods (bispectrum, trispectrum,...) designed to restore those nonlinearity-contributed high-frequency spectral energy to the base frequency. It is fair to say that

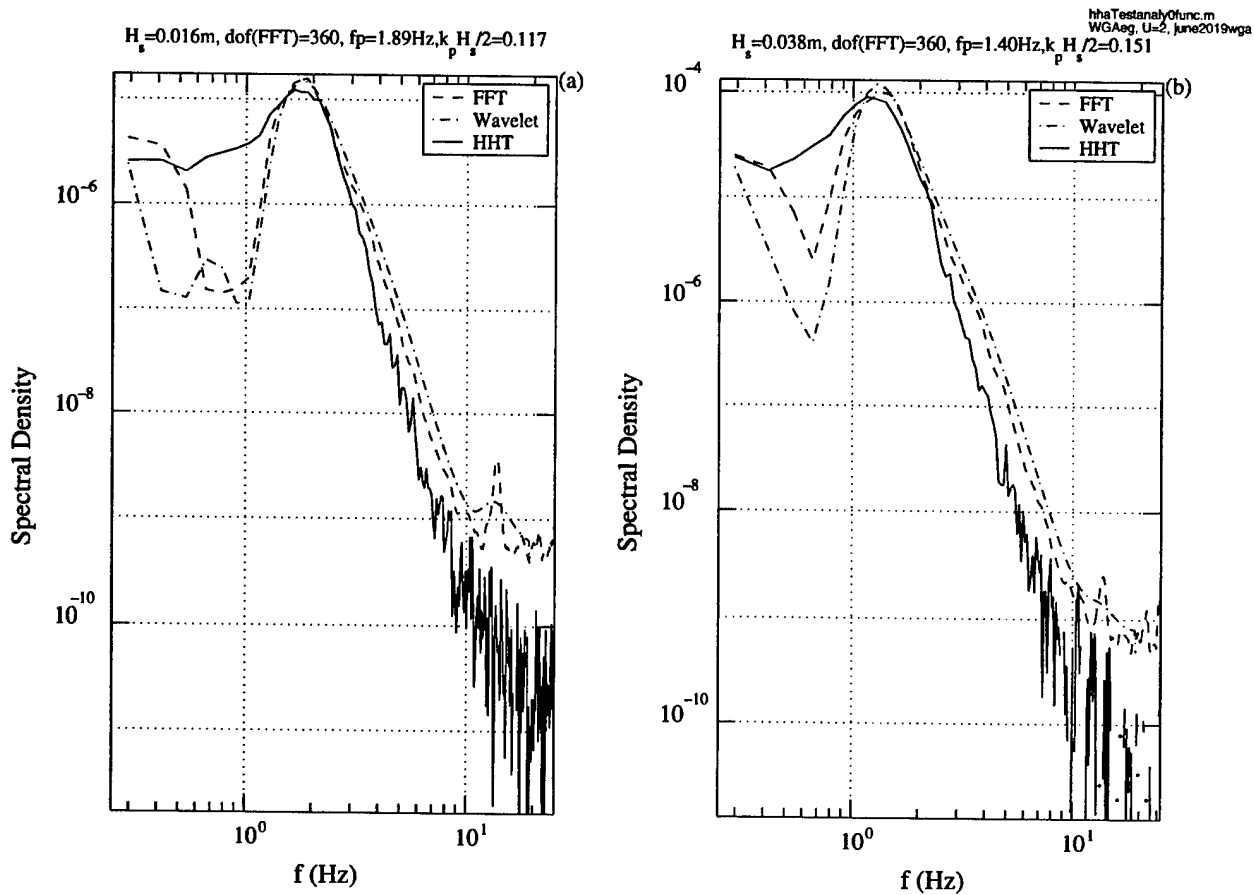


Fig. 5. Spectra of wind-generated waves. The average wind speed is (a) 2 m s^{-1} and (b) 5 m s^{-1} .

Fourier-based methods always overestimate the spectral level at frequencies higher than the spectral peak. The HHT interprets wave nonlinearity in terms of frequency modulation and the spectral energy of a nonlinear wave remains at the neighborhood of the base frequency (see also Fig. 3d).

Fig. 6a shows the ratio of the spectral densities, S_F/S_H and S_w/S_H , where subscripts F, H, and w are for FFT, HHT, and wavelet, respectively. Using the HHT spectrum as reference, the spectral density derived from Fourier-based analysis is in general much lower (by a factor of about 80 at its minimal point) at low frequencies and much higher (by about a factor of 10) at high frequencies. We also processed the spectral difference normalized by the peak spectral density, $(S_F - S_H)/S_H(f_p)$ and $(S_w - S_H)/S_H(f_p)$. The results are shown in Fig. 6b. Significant differences in the spectral properties are obvious in the frequency region lower than the second harmonic of the peak frequency. These differences in the frequency distribution of wave energy certainly have impacts on ocean engineering designs. For example, the mean frequency as defined by the normalized first moment of wave spectrum, $f_1 = \int fS(f) df / \int S(f) df$, is 13% lower in the HHT spectrum than that of the Fourier spectrum, and 21% lower than that of the wavelet spectrum for the examples shown in Fig. 5. These results suggest that

the design wave spectrum presently used in engineering applications may underestimate the low frequency impact of wave motion.

4. Summary

Analyzing nonlinear and nonstationary signals remains a very challenging task. Presently, most methods developed to deal with nonstationarity are based on the concept of Fourier decomposition; therefore all the shortcomings associated with Fourier transformation are inherent in those methods also. The recent introduction of EMD by Huang et al. [1,2] represents a fundamentally different approach for decomposing nonlinear and nonstationary signals. The associated spectral analysis (HHT) provides superior spatial (temporal) and wavenumber (frequency) resolution for handling nonstationarity and nonlinearity (Section 2). The HHT spectrum also results in a considerably different interpretation of nonlinearity (frequency modulation). Applying the technique to the problems of wind generated ocean waves, we found that the spectral function derived from HHT is markedly different from those obtained by the Fourier-based techniques. The difference in the resulting spectral functions is attributed to

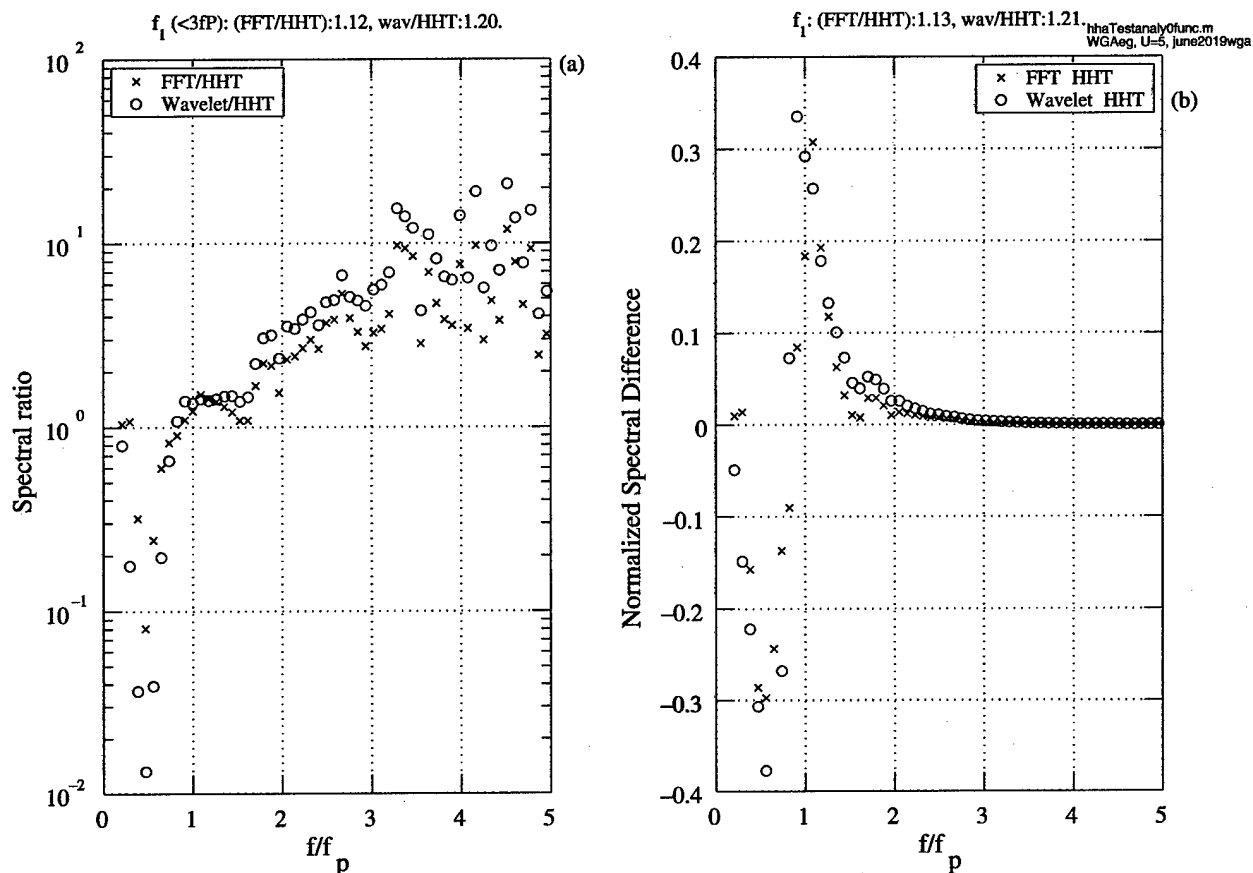


Fig. 6. (a) The ratios of wavelet and Fourier spectra normalized by the HHT spectrum. (b) The difference spectra normalized by the HHT peak spectral density. The average wind speed is 5 m s^{-1} . Similar results are found for 2 m s^{-1} wind condition.

the interpretation of nonlinearity. The Fourier techniques decompose a nonlinear signal into sinusoidal harmonics; therefore some of the spectral energy at the base frequency is distributed to the higher frequency components. The HHT interprets nonlinearity in terms of frequency modulation and the spectral energy remains in the neighborhood of the base frequency. This results in a considerably higher spectral energy at lower frequencies and sharper dropoff at higher frequencies in the HHT spectrum in comparison with the Fourier-based spectra. The mean frequency computed from HHT spectrum is 13–21% lower than those derived from Fourier-based spectra. These results suggest that the design wave spectrum presently in use may underestimate the low frequency impact of wave motion, and that the mean frequency of random wave motion is lower than that estimated by a standard design wave spectrum by about 20%.

Acknowledgements

This work is supported by the Office of Naval Research (Naval Research Laboratory Program Elements N61153

and N62435, PAH and DWW) and NASA RTOP program on micro-scale ocean dynamics (NEH). This is NRL contribution JA/7330-02-0078.

References

- [1] Huang NE, Shen Z, Long SR, Wu MC, Shih HH, Zheng Q, Yuen NC, Tung CC, Liu HH. The empirical mode decomposition and the Hilbert spectrum for nonlinear and nonstationary time series analysis. *Proc R Soc Lond* 1998;454A:903–95.
- [2] Huang NE, Shen Z, Long SR. A new view of nonlinear water waves: the Hilbert spectrum. *Annu Rev Fluid Mech* 1999;31:417–57.
- [3] Huang NE, Wu ML, Long SR, Shen SS, Qu WD, Gloersen P, Fan KL. A confidence limit for the empirical mode decomposition and Hilbert spectral analysis. *Proc R Soc Lond* 2003;459A:2317–45.
- [4] Melville WK. Wave modulation and breakdown. *J Fluid Mech* 1983; 128:489–506.
- [5] Bitner-Gregersen EM, Gran S. Local properties of sea waves derived from a wave record. *Appl Ocean Res* 1983;5:210–4.
- [6] Hwang PA, Xu D, Wu J. Breaking of wind-generated waves: measurements and characteristics. *J Fluid Mech* 1989;202:177–200.
- [7] Chapman RD, Monaldo FM. The APL wave gauge system. Rep. S1R-91U-041, Baltimore, MD: Applied Physics Laboratory, The Johns Hopkins University; 1991. 25 pp.